J. Agr. Sci. Tech. (2009) Vol. 11: 457-468

A 2D Numerical Depth-averaged Model for Unsteady Flow in Open Channel Bends

M. M. Ahmadi[1], S. A. Ayyoubzadeh[1]*, M. Montazeri Namin[2], and J. M. V. Samani[1]

ABSTRACT

The purpose of this paper is to present a 2D depth-averaged model for simulating and examining unsteady flow patterns in open channel bends. In particular, this paper proposes a 2D depth-averaged model that takes into account the influence of the secondary flow phenomenon through calculation of the dispersion stresses. The dispersion terms which arose from the integration of the product of the discrepancy between the mean and the actual vertical velocity distribution were included in the momentum equations in order to take into account the effect of the secondary current. This model used a time-splitting method for solving advection, diffusion and other momentum equation terms. The proposed model uses an orthogonal curvilinear coordinate system efficiently and accurately to simulate the flow field with irregular boundaries; it also used a finite volume projection method approach for solving the governing equation in a staggered grid. Two sets of experimental data were used to demonstrate the model's capabilities. The comparison of the simulated water surface elevation with the measurements shows good agreement and indicates that inclusion of the dispersion terms improved the simulation results.

Keywords: Bend, Meander, Numerical models, Open channels, Two dimensional model, Unsteady flow.

INTRODUCTION

Flow in Meanders

Flow characteristics in meandering channels are much more complicated than those in straight reaches. Due to the secondary flow, flow passing through a meandering channel is of a three-dimensional nature.

Secondary flow results from the imbalance between the transverse water surface gradient force and centrifugal force over the depth due to the vertical variation of the primary flow velocity. In other words, the inward pressure gradient near the bed prevails over the centrifugal force resulting in an inward flow along the bed and outward flow near the water surface.

Pioneering investigation of the flow phenomena in open channel bends is generally attributed to Thompson (1876) who observed the spiral motion inherent in a channel bend by introducing seeds and dyes into the flow. Since then, many studies have been conducted on flows in bends (e.g., Mockmore, 1943; Shukhry, 1949; Rozovskii, 1961; Yen, 1965).

To simulate flow accurately in meandering channels, flow passing through meandering channels requires a 3D hydrodynamic model. Many 3D numerical models have been developed (Leschziner and Rodi, 1979; Sinha *et al*., 1998; Wu *et al.*, 2000) to simulate the complicated spiral flow motion in river bends. When dealing with practical

[1] Department of Water Structures Engineering, College of Agriculture, Tarbiat Modares University, P. O. Box: 14115-336, Tehran, Islamic Republic of Iran.
[2]Department of Civil Engineering, Tehran University, Tehran, Islamic Republic of Iran.
* Corresponding author, e-mail: ayyoub@modares.ac.ir

[DOR: 20.1001.1.16807073.2009.11.4.8.3]

engineering problems, such as alluvial geomorphic processes, it is not computationally efficient to use 3D models. Instead, researchers (Howard, 1984; Smith, 1984; Johannesson and Parker, 1989 a, b; Nelson and Smith, 1989; Odgaard, 1989; Shimizu *et al.*, 1990; Molls and Chaudhry, 1995; Ye and McCorquodale, 1997; Lien *et al.*, 1999; Darby *et al.*, 2002; Hsieh and Yang, 2003) applied two dimensional (2D) models to simulate meandering channel flow.

The 2D depth-averaged models used can be classified into two types, the conventional model and the bend-flow model (Hsieh and Yang, 2003). The major difference between the two is the treatment of dispersion stress terms in the momentum equations. Integrating along the vertical direction of velocity from the depth-averaged values represents the dispersion stress terms. The conventional model assumes that vertical velocity is uniform while the secondary current effect is ignored. On the other hand, the bend flow model takes into account the influence of the dispersion stress terms arising from the integration of the products of the discrepancy between the mean and the adopted secondary-current velocity distribution.

Conventional models have been widely used by many researchers. Molls and Chaudhry (1995) proposed the concept of interacting effective stresses, which consists of the laminar viscosity stresses and the turbulent stresses, to simulate the experimental bend-flow data reported by Rozovskii (1961).

Ye and McCorquodale (1997) proposed a fractional two-step implicit model to simulate the experimental bend-flow data reported by Chang (1988). Ye and McCorquodale (1997) and Bui Minh (2004) increased the coefficient of exchange of momentum in a horizontal direction (i.e. the effective eddy viscosity) to account for the effects of the secondary motion. For the same reason, when using conventional models to simulate mass transport, it is necessary to reduce the Schmidt number to correct the dispersion effects (Ye and McCorquodale, 1997; Duan, 2004). Although this simulation showed good agreement compared to the experiment data, conventional models are not adequate for mass transport in curved channels since the Schmidt number varies over a wide range and requires calibration.

Flokestra (1977) indicated the need for dispersion stress terms for bend flow simulation. Finnie *et al.* (1999) later followed Flagstar's concept to solve a transport equation for streamwise vortices and incorporated the so-called associated acceleration terms, i.e., dispersion stress terms, to the depth-averaged equations. The inclusion of these acceleration terms results in improved predictions of depth-averaged velocity in bend-flow simulation. Lien *et al.* (1999) further showed that the simulated results without considering the dispersion stress terms are consistent with the potential theory, in which the velocity distribution is skewed inwards and away from the sidewalls and approaches to the free-vortex distribution.

Hsieh and Yang (2003) studied the suitability of 2D models for bend flow simulation by using both a conventional model and a bend-flow model. Analysis of the simulation results indicated that the maximum relative difference in longitudinal velocity is mainly related to the relative strength of the secondary current and the relative length of the channel. Empirical relations connecting the maximum relative difference in longitudinal velocities, the relative strength of the secondary current, and the relative length of the channel, were all proposed to be used as a guideline for model users.

The purpose of this paper is to present an unsteady 2D depth-averaged flow model taking into consideration the dispersion stress terms to simulate the bend flow field. The model uses an orthogonal curvilinear coordinate system efficiently to simulate the flow field with an irregular boundary. Numerically, the proposed model employs projection and time-splitting methods for solving the flow governing equations. Two sets of experimental data measured by de

[DOR: 20.1001.1.16807073.2009.11.4.8.3]

Vriend (1979) and Rozovskii (1961) are used to examine the capabilities of the proposed model.

METHODOLOGY

Flow Simulation

Depth-Averaged Equations in Orthogonal Curvilinear Coordinates

Under the assumption of incompressible fluid, constant viscosity, and hydrostatic pressure distribution over the depth, the depth-averaged equations can be obtained from integrating the Navier-Stokes equation along water depth using the kinematics boundary conditions. The unsteady 2D depth-averaged flow governing equations including the basic continuity [Equation (1)] and momentum equations [Equations (2) and (3)] can, respectively, be written in orthogonal curvilinear (s, n) coordinates as follows (Thein, 1994) :

the Continuity equation:

$$\frac{\partial \xi}{\partial t}+\frac{\partial p}{\partial s}+\frac{\partial q}{\partial n}-\frac{q}{R_s}+\frac{p}{R_n}=0 \qquad (1)$$

and the Momentum equation in *s*-direction:

$$\frac{\partial p}{\partial t}+\frac{\partial}{\partial s}(\bar{u}p)+\frac{\partial}{\partial n}(\bar{v}p)-2\frac{pq}{hR_s}+\frac{p^2-q^2}{hR_n}+\frac{\partial D_{uu}}{\partial s}+\frac{\partial D_{uv}}{\partial n}+\tau_{bs}+gh\frac{\partial \xi}{\partial s}=\frac{\partial}{\partial s}\left(E\frac{\partial p}{\partial s}\right)+\frac{\partial}{\partial n}\left(E\frac{\partial p}{\partial n}\right)-\frac{2E}{R_s}\frac{\partial q}{\partial s}-\frac{2E}{R_n}\frac{\partial q}{\partial n}-\frac{\partial E}{\partial s}\frac{q}{R_s}-\frac{\partial E}{\partial n}\frac{q}{R_n} \qquad (2)$$

and in *n*-direction:

$$\frac{\partial q}{\partial t}+\frac{\partial}{\partial s}(\bar{u}q)+\frac{\partial}{\partial n}(\bar{v}q)+2\frac{pq}{hR_n}+\frac{p^2-q^2}{hR_s}+\tau_{bn}+\frac{\partial D_{vv}}{\partial n}+\frac{\partial D_{uv}}{\partial s}+gh\frac{\partial \xi}{\partial n}=\frac{\partial}{\partial s}\left(E\frac{\partial q}{\partial s}\right)+\frac{\partial}{\partial n}\left(E\frac{\partial q}{\partial n}\right)+\frac{2E}{R_s}\frac{\partial p}{\partial s}+\frac{2E}{R_n}\frac{\partial p}{\partial n}+\frac{\partial E}{\partial s}\frac{p}{R_s}+\frac{\partial E}{\partial n}\frac{p}{R_n} \qquad (3)$$

where $p= uh$ and $q= vh$ are mass fluxes in the s and n directions, respectively; τ_{bs}, τ_{bn} are the components of the bed-shear stress in the s and n direction that can be written as follows:

$$\tau_{bs}=\frac{gp\sqrt{p^2+q^2}}{C^2h^2} \qquad (4)$$

$$\tau_{bn}=\frac{gq\sqrt{p^2+q^2}}{C^2h^2} \qquad (5)$$

where s and n are orthogonal curvilinear coordinates in the streamwise and transverse axes, respectively; $\bar{u}$ and $\bar{v}$ are depth-averaged velocity components in s and n directions, respectively; t is time; ξ is water surface elevation; h is flow depth; R_s and R_n are radius of curvature of the s and n axes, respectively; C is the Chezy coefficient; E is the eddy viscosity coefficient and D_{uu}, D_{vv}, D_{uv} are dispersion terms, their expressions are as follows:

$$D_{uu}=\int_{z_b}^{z_b+h}(u-\bar{u})^2\,dz$$

$$D_{uv}=\int_{z_b}^{z_b+h}(u-\bar{u})(v-\bar{v})\,dz \qquad (6)$$

$$D_{vv}=\int_{z_b}^{z_b+h}(v-\bar{v})^2\,dz$$

where z_b bed elevation and u and v are velocity components in the streamwise and transverse directions, respectively.

Turbulence Model

In this model, the Smagorinsky viscosity formulation with the following expression is adopted:

$$E=C_s^2\Delta^2\sqrt{\left(\frac{\partial \bar{u}}{\partial x}\right)^2+\left(\frac{\partial \bar{v}}{\partial y}\right)^2+\left(\frac{\partial \bar{u}}{\partial y}+\frac{\partial \bar{v}}{\partial x}\right)^2} \qquad (7)$$

where Δ is grid spacing and C_s is a constant to be chosen in the interval of 0.25 to 1.0 (Brandt, 2006).

[DOR: 20.1001.1.16807073.2009.11.4.8.3]

Dispersion Terms in the Momentum Equations

Because of the secondary flow, the integration of the product of the discrepancy between the depth-averaged and the actual velocity can no longer be neglected. In this model, the velocity profiles in the streamwise and transverse directions proposed by de Vriend (1977) and Rozovskii (1961) are adopted, respectively:

$$u = \bar{u}\left(1 + \frac{\sqrt{g}}{\kappa C} + \frac{\sqrt{g}}{\kappa C}\ln\zeta\right) = \bar{u} f_m(\zeta) \quad (8)$$

$$v = \bar{v} f_m(\zeta) + \frac{\bar{u}h}{\kappa^2 R_s}\left\{F_1(\zeta) - \frac{\sqrt{g}}{\kappa C}\left[F_2(\zeta) + 0.8(1+\ln\zeta)\right]\right\} \quad (9)$$

in which

$$f_m(\zeta) = 1 + \frac{\sqrt{g}}{\kappa C} + \frac{\sqrt{g}}{\kappa C}\ln\zeta \quad (10)$$

$$F_1(\zeta) = \int \frac{2\ln\zeta}{\zeta - 1} d\zeta \quad (11)$$

$$F_2(\zeta) = \int \frac{\ln^2\zeta}{\zeta - 1} d\zeta \quad (12)$$

where $\zeta = (z - z_b)/h$ is dimensionless distance from the bed, z_b is bed elevation, C is the Chezy coefficient, g is the gravitational acceleration and κ is the Von Karman constant.

According to Equations (8) and (9), the primary velocity profile is assumed to follow a logarithmic distribution, and the transverse velocity profiles are a combination of the secondary flow. It is obvious that only the secondary flow due to the curvature of the bend is considered in the formulation of the transverse velocity profile. Such a consideration of transverse secondary flow is a main factor in shifting the streamwise momentum from the inner region of a bend towards the outer region and to increase the main velocity near the outer bank. In this simulation, the effect of the secondary flow on the vertical distribution of streamwise velocity and also the local secondary flow that may occur near the surface at the outer bank have been neglected. Substituting Equations (8) and (9) into Equation (6) yields:

$$D^c_{uu} = \bar{u}^2 h\left(\frac{\sqrt{g}}{\kappa C}\right)^2 \quad (13)$$

$$D^c_{vv} = h\bar{v}^2\left(\frac{\sqrt{g}}{\kappa C}\right)^2 + \frac{\bar{u}^2 h^3}{\kappa^4 R_s^2} FF_2 + \frac{2\bar{u}\bar{v}h^2}{\kappa^2 R_s}\left(\frac{\sqrt{g}}{\kappa C}\right) FF_1 \quad (14)$$

$$D^c_{uv} = h\bar{u}\bar{v}\left(\frac{\sqrt{g}}{\kappa C}\right)^2 + \frac{\bar{u}^2 h^2}{\kappa^2 R_s}\left(\frac{\sqrt{g}}{\kappa C}\right) FF_1 \quad (15)$$

These dispersion terms have been included in Equations (2) and (3) to solve flow velocity,

$$FF_1 = \int_0^1 (1+\ln\zeta)\left(F_1(\zeta) - \frac{\sqrt{g}}{\kappa C} F_4(\zeta)\right) d\zeta \quad (16)$$

$$FF_2 = \int_0^1 \left[F_1(\zeta) - \frac{\sqrt{g}}{\kappa C} F_4(\zeta)\right]^2 d\zeta \quad (17)$$

where $F_4(\zeta) = \left(F_2(\zeta) + 0.8(1+\ln\zeta)\right)$. Note that Equations (15) and (16) can be integrated numerically using the trapezoidal rule.

Numerical Algorithm

The present model used a finite volume projection method approach (Temam, 1991; Mohammadzadeh Ghomi and Montazeri Namin, 2005) for solving the governing equation in a staggered grid. The key feature of this method is to solve the governing equation in three steps. The first step is to compute the mass fluxes (p and q) in the momentum equations without considering the pressure terms and continuity equation. The second step is to compute the water

[DOR: 20.1001.1.16807073.2009.11.4.8.3]

elevation with the implicit scheme in two stages. The first stage is to compute the water elevation in time step t+1/2 by solving the continuity equation and pressure term Equation (18) remaining from the momentum equations in s direction where time step t+1/2 denotes the intermediate step between t and t+1. The second stage of the second step is to compute water elevation in time step t+1 by solving the continuity equation and pressure term Equation (19) remaining from the momentum equations in n direction.

$$\frac{\partial p}{\partial t} + gh\frac{\partial \xi}{\partial s} = 0.0 \tag{18}$$

$$\frac{\partial q}{\partial t} + gh\frac{\partial \xi}{\partial n} = 0.0 \tag{19}$$

The last step is to modify the provisional mass fluxes using the water elevation value and Equations (17) and (18). They are expressed sequentially as follows:

First Step:

$$\begin{aligned}
&\frac{p_{j,k}^{t+1/2} - p_{j,k}^{t}}{\Delta t} + \frac{(\overline{u}p)_{j-1/2,k}^{t} - (\overline{u}p)_{j+1/2,k}^{t}}{\Delta s_{j,k}} + \\
&\frac{(\overline{v}p)_{j,k+1/2}^{t} - (\overline{v}p)_{j,k-1/2}^{t}}{\Delta n_{j,k}} - 2(\frac{q}{hR_s})_{j,k}^{t} p_{j,k}^{t+1} + \\
&\frac{p_{j,k}^{t+1/2} p_{j,k}^{t} - (q_{j,k}^{t})^2}{(hR_n)_{j,k}^{t}} + \frac{(D_{uu}^{c})_{j+1/2,k}^{t} - (D_{uu}^{c})_{j-1/2,k}^{t}}{\Delta s_{j,k}} \\
&+ \frac{(D_{uv}^{c})_{j,k+1/2}^{t} - (D_{uv}^{c})_{j,k-1/2}^{t}}{\Delta n_{j,k}} + \\
&(\frac{gn_m^2\sqrt{p^2+q^2}}{h^{7/3}})_{j,k}^{t} p_{j,k}^{t+1/2} = \\
&\frac{\left(E\frac{\partial p}{\partial s}\right)_{j+1/2,k}^{t} - \left(E\frac{\partial p}{\partial s}\right)_{j-1/2,k}^{t}}{\Delta s_{j,k}} + \\
&\frac{\left(E\frac{\partial p}{\partial n}\right)_{j,k+1/2}^{t} - \left(E\frac{\partial p}{\partial n}\right)_{j,k-1/2}^{t}}{\Delta n_{j,k}} - \\
&(\frac{2E}{R_s})_{j,k}^{t} \frac{q_{j+1/2,k}^{t} - q_{j-1/2,k}^{t}}{\Delta s_{j,k}} - (\frac{2E}{R_n})_{j,k} \frac{q_{j,k+1/2}^{t} - q_{j,k-1/2}^{t}}{\Delta n_{j,k}} - \\
&(\frac{q}{R_s})_{j,k}^{t} \frac{E_{j+1/2,k}^{t} - E_{j-1/2,k}^{t}}{\Delta s_{j,k}} - (\frac{q}{R_n})_{j,k}^{t} \frac{E_{j,k+1/2}^{t} - E_{j,k-1/2}^{t}}{\Delta n_{j,k}}
\end{aligned} \tag{20}$$

Similarly, the difference form of mass flux component in direction n can be derived from Equation (3). Superscript t denotes the known variables at time step t, and superscript t+1 denotes the unknown variables at time step t+1. Subscript j, k denotes the variables position in s and n directions, respectively, in the computational domain.

The first step includes convection, diffusion, dispersion and resistance terms in the momentum equations accompanied by additional terms in this equation due to the curving grid line. This model used the time-splitting method (Kin and Moin, 1985; Rowinski, Dysarz and Napiorkowski, 2004) for solving momentum equations' terms. In this method it has been assumed that the influence of different processes might best be computed separately as several stages in a several different schemes. It is important to note that, at the next stage the input for the computations is taken from the first process and not from the actual preceding time level. In the first step, the advection and diffusion terms in the momentum equations are solved using the second order explicit Fromm and implicit schemes, respectively. Other terms in these equations are solved using the implicit scheme. At the next step, mass fluxes $p^{t+1/2}, q^{t+1/2}$ are computed using Equations (22) and (23).

Second Step, First Stage

From the continuity equation:

$$\begin{aligned}
&\frac{\xi_{j,k}^{t+1/2} - \xi_{j,k}^{t}}{0.5\Delta t} + \frac{(p_{j+1/2,k}^{t+1} - p_{j-1/2,k}^{t+1})}{\Delta s_{j,k}} + \\
&\frac{(q_{j,k+1/2}^{t} - q_{j,k-1/2}^{t})}{\Delta n_{j,k}} - \frac{q_{j,k}^{t}}{Rs_{j,k}} + \frac{p_{j,k}^{t+1}}{Rn_{j,k}} = 0
\end{aligned} \tag{21}$$

using Equation (18)

$$\begin{aligned}
p_{j+1/2,k}^{t+1} = [\, &p_{j+1/2,k}^{t+1/2} - \\
&gh_{j+1/2,k}^{t} \frac{\Delta t}{\Delta s_{j,k}} (\xi_{j+1,k}^{t+1/2} - \xi_{j,k}^{t+1/2})]
\end{aligned} \tag{22}$$

[DOR: 20.1001.1.16807073.2009.11.4.8.3]

$$p_{j-1/2,k}^{t+1} = [p_{j-1/2,k}^{t+1/2} - gh_{j-1/2,k}^{t} \frac{\Delta t}{\Delta s_{j,k}} (\xi_{j,k}^{t+1/2} - \xi_{j-1,k}^{t+1/2})] \quad (23)$$

Water elevation in time step t+1/2 i.e. $\xi^{t+1/2}$ is computed by substituting Equations (22) and (23) into Equation (21).

Second Step, Second Stage

From the continuity equation:

$$\frac{\xi_{j,k}^{t+1} - \xi_{j,k}^{t+1/2}}{0.5\Delta t} + \frac{(p_{j+1/2,k}^{t} - p_{j-1/2,k}^{t})}{\Delta s_{j,k}} + \frac{(q_{j,k+1/2}^{t+1} - q_{j,k-1/2}^{t+1})}{\Delta n_{j,k}} - \frac{q_{j,k}^{t+1}}{Rs_{j,k}} + \frac{p_{j,k}^{t}}{Rn_{j,k}} = 0 \quad (24)$$

using Equation (18)

$$q_{j,k+1/2}^{t+1} = [q_{j,k+1/2}^{t+1/2} - gh_{j,k+1/2}^{t} \frac{\Delta t}{\Delta n_{j,k}} (\xi_{j,k+1}^{n+1} - \xi_{j,k}^{n+1})] \quad (25)$$

$$q_{j,k-1/2}^{t+1} = [q_{j,k-1/2}^{t+1/2} - gh_{j,k-1/2}^{t} \frac{\Delta t}{\Delta n_{j,k}} (\xi_{j,k}^{t+1} - \xi_{j,k-1}^{t+1})] \quad (26)$$

Water elevation in time step t +1, ξ^{t+1} is computed by substituting Equations (25) and (26) into Equation (24).

Last Step

Using Equations (21), (22), (24) and (25) through water elevation in time step t+*1*, mass fluxes p and q in time step n+1 are computed.

Boundary Conditions

Three types of boundaries -the inlet or upstream end, outlet or downstream end, and solid walls- are considered. The discharge hydrograph per unit width can be specified at the inlet section. Water surface elevation can be specified at the outlet section. At the solid boundaries the flow velocity is assumed to be zero.

RESULTS

Model Verification

To test and verify the performance and

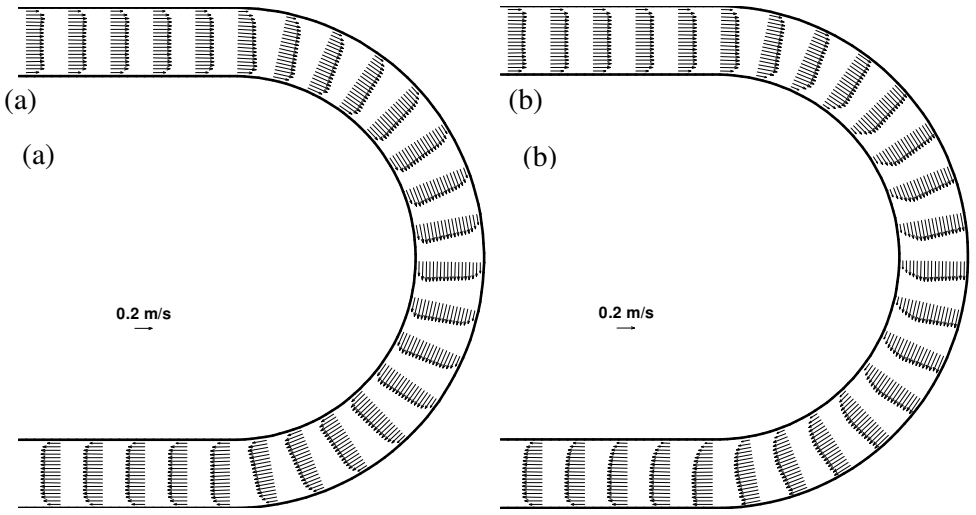

Figure 1. Velocity redistribution by numerical simulation for mild curve: (a) Ignoring secondary flow; (b) Taking secondary flow into account.

[DOR: 20.1001.1.16807073.2009.11.4.8.3]

Table1. Channel geometry and flow parameters of simulated cases.

Case	Discharge Q (m^3 s^{-1})	Width B (m)	Depth d (m)	Velocity V (m s^{-1})	R/B
de Vriend (1979)	0.0671	1.7	0.1953	0.202	3.5
Rozovskii (1961)	0.0123	0.8	0.053	0.265	1.0

capabilities of the proposed model, two sets of experimental data on bend flow conducted by de Vriend (1979) and Rozovskii (1961) are adopted. These selected channels belong to mildly curved and sharply curved channels, respectively. Data regarding the channel dimensions and flow conditions are summarized in Table 1.

Flow in a Mildly Curved Channel

In de Vriend's (1979) experiment, the channel consists of a 1.7 m wide flume with a U-shaped plan. With a horizontal bottom and vertical sidewalls, the radius of curvature of the flume axis in the bend is 4.25 m and the upstream and downstream straight reaches have an effective length of about 6.0 m. The ratio of radius of curvature to channel width is 3.5. The discharge at the inlet is 0.0671 m^3 s^{-1}. The averaged velocity is 0.202 m s^{-1}, and the average flow depth is 0.1953 m.

Figure 1a shows the velocity redistribution across the channel width along the bend, ignoring the dispersion stresses. The simulated results are consistent with the potential theory by which the velocity is inversely proportional to the radius of the curvature. Hence, the flow velocity along the channel bend is higher in the inner bank region than that in the outer bank region, as clearly shown in Figure 1a while the flow velocity at the inner and outer banks are almost equal at the inlet of the bend.

If the dispersion stresses are included in the bend flow simulation, they act as a sink or source in the momentum equation, which cause the transverse convection of momentum to shift from the inner bank to the outer bank (Kalkwijk and de Vriend, 1980; de Vriend, 1981). Figure 1b shows the simulated results with dispersion stress, which clearly demonstrate a shift of the maximum main velocity along the channel bend from the inner bank region towards the outer bank region. However, for this mild

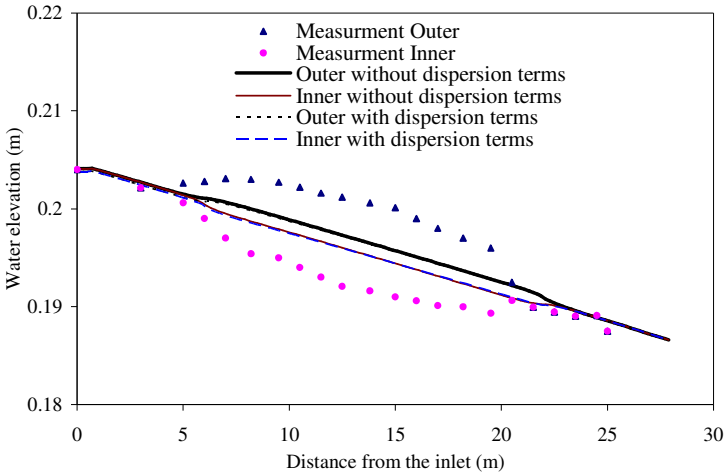

Figure 2. Comparison between sidewall flow depth, ignoring and taking secondary flow into account; mildly curved channel.

[DOR: 20.1001.1.16807073.2009.11.4.8.3]

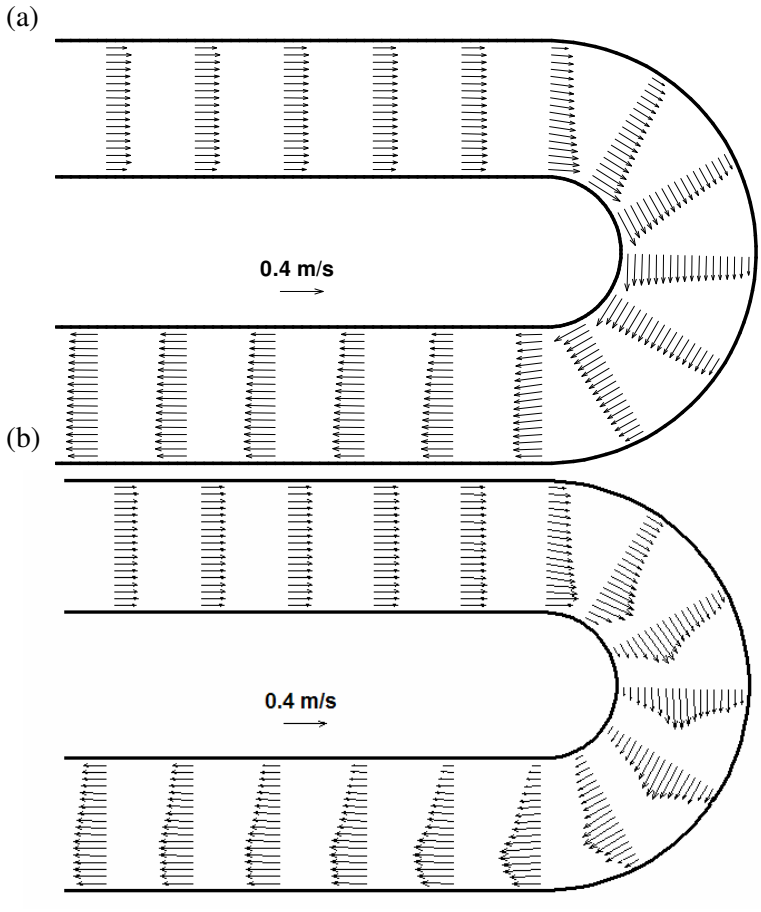

Figure 3. Velocity redistribution by numerical simulation for sharply curved channel: (a) Ignoring secondary flow; (b) Taking secondary flow into account.

bend, the radius of channel curvature is much larger than the width of the channel and thus the effect of secondary flow is very weak.

The comparison of simulated water surface elevation with the measurement at the inner bank and outer bank for the cases with or without the dispersion terms is plotted in Figure 2. It is shown that the water surface elevation at the outer bank is at much higher level than that in the inner bank throughout the bend. The rise of flow at the outer bank results from the centrifugal force. One also can discern a small difference between the result with and without the dispersion terms. In general, the simulated water elevations are in agreement with the measurement at the inner and outer banks, separately. The difference between the simulated results with and without secondary flow is not significant because the secondary flow effect in a mild bend is weak.

Flow in a Sharply Curved Channel

The present 2D model was also applied to the experimental results obtained by Rozovskii (1961) in a sharply curved flume. The flume includes a 180 curved reach with a 6 m long straight approach and a 3 m long straight exit. The ratio of mean radius of curvature to width is 1.0; the width of the channel is 0.8 m. The cross section of the bend is rectangular and connected to the straight inlet and outlet reaches of the same

[DOR: 20.1001.1.16807073.2009.11.4.8.3]

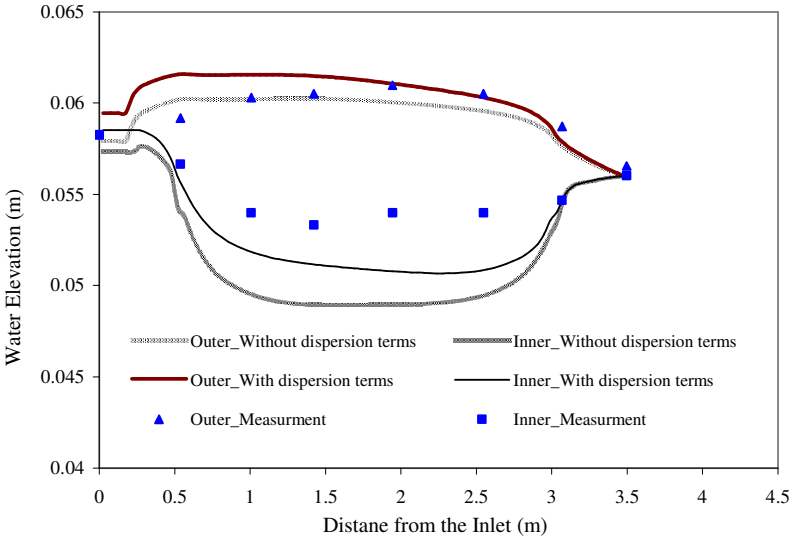

Figure 4. Comparison between sidewall flow depth in the cases of ignoring and taking secondary flow into account; sharply curved channel.

cross section. Water depth at the downstream end is 0.053 m, and the discharge is 0.0123 m s^{-1}.

Figure 3a and 3b show the computed velocity distribution across the channel width with and without secondary flow effects, respectively. As shown in Figure 3a, the velocity at the inner bank becomes larger while that at the outer bank becomes smaller when the flow enters the bend. Such a flow pattern prevails through of the entire bend. The simulated velocity distribution becomes relatively uniform after some distance downstream of the bend exit. When considering the secondary flow effect, Figure 3b indicates different velocity distributions after the flow enters the bend. In this situation, the maximum main velocity along the channel bend shifts from the inner bank region towards the outer bank region.

Figure 3b shows that the velocity distribution with the secondary flow effect is no longer uniform in the straight channel even after the flow exits the bend. The velocity near the outer bank region abruptly speeds up, and the corresponding velocity near the inner bank region decelerates. This phenomenon can be explained by the decline of the transverse slope of the water surface and the release of the remaining additional momentum by the secondary flow effect when the radius of curvature at the bend exit abruptly changes to infinity.

Figure 4 shows the comparison of simulated surface elevation with and without the dispersion terms along the channel length. It can be seen that, along the bend, the water level rises at the outer bank and falls at the inner bank. We should note that, without the secondary flow effect, the water level will be underestimated at the outer bank. Furthermore, the consideration of the secondary flow effect and decrease in the slope of super elevation between the inner bank and outer bank is observed in the measured data.

This result showed that the impact of secondary flow on the depth-averaged flow distribution and water surface elevations becomes more visible with increasing channel curvature.

[DOR: 20.1001.1.16807073.2009.11.4.8.3]

CONCLUSIONS

This paper presents an unsteady 2D depth-averaged model developed using an orthogonal curvilinear coordinate system. The model takes into account vertical velocity profiles in a bend, using them to capture the effect of dispersion stress on the floor. Dispersion stress terms serve as a sink or source in the momentum and conservation equations are needed to calculate the transverse convection of momentum caused by the secondary flow along a channel bend (Kalkwijk and de Vriend, 1980; de Vriend, 1981). If the dispersion stress terms are neglected, the governing equations reduce to a conventional depth-averaged equation assuming uniform velocity over depth. In other words, the model presented here should be more applicable for practical application in bend flow modeling than conventional depth- averaged models because of its ability to account for the secondary flow effect.

Two sets of experimental bend-flow data, one with mild bends and the other with sharp bends, were used to demonstrate the capabilities of the proposed model. The simulated water elevation results and experimental data agree well in both cases of the mildly and sharp curved channels and the computed results show that the secondary flow effect has been properly represented by calculating the dispersion stresses. In short, the dispersion stresses play an important role in accurately simulating or predicting flow fields in sharp bends as well as in mild bends.

REFERENCES

1. Brandt, T. T. 2006. Study of Large Eddy Simulation and Smagorinsky Model using Explicit Filtering. 36th AIAA Fluid Dynamics Conference and Exhibit, 5-8 June 2006, San Francisco, California
2. Bui Minh, D. 2004. Numerical Modeling of Bed Deformation in Laboratory Channels. *J. hydraul. Eng., ASCE,* 130**(9):** 894-904.
3. Chang, H. H. 1988. Processes of Meander Bend Migration, Discussion of Effect of Flow Paths on Migration of Symmetrical Meanders, In: *"Proceedings 1988, ASCE Conference*". Abt, S. R. and Gessler, J. (Eds.), *Hydrol. Eng.,* PP. 690-695.
4. Darby, S. E., Alabyan, A. M. and Van de Weil, M. J. 2002. Numerical Simulation of Bank Erosion and Channel Migration in Meandering Rivers, *Water Resour. Res.*, **38(9):** 2-12.
5. de Vriend, H. 1977. A Mathematical Model of Steady Flow in Curved Shallow Channel. *J. Hydraul. Res.*, **15(1)**: 37-54.
6. de Vriend, H. 1979. Flow Measurement in a Curved Rectangular Channel. Internal Report, No. 9-97. Tech. Rep., Laboratory of Fluid Mechanics, Depth. Of Civil Engineering, Delft Univ. of Technology, Delft, The Netherlands.
7. de Vriend, H. 1980. Velocity Redistribution in Curved Rectangular Channels. *J. Fluid Mech.*, **107**: 423-439.
8. de Vriend, H. 1981. Flow Measurement in a Curved Rectangular Channel. Part 2: Rough Bottom. Internal Report, No. 5-81. Tech. Rep., Laboratory of Fluid Mechanics, Depth. Of Civil Engineering, Delft Univ. of technology, Delft, The Netherlands.
9. Duan, J. G. 2004. Simulation of Flow and Mass Dispersion in Meandering Channels, *J. Hydraul. Eng.*, *ASCE*, **130(10)**: 964-976.
10. Finnie, J. Donnell, B., Letter, J., Bernard R. S. 1999. Secondary flow correction for depth-Averaged flow calculation, *J. Hydrol. Mech.*, **125(7):** 848-858.
11. Flokestra, C. 1977. The Closure Problem for Depth Averaged two Dimensional Flows, *Proc. 18th Congress of the int. Association for Hydraul. Res.,* PP. 247-256.
12. Howard, A. 1984. *Simulation Model of Meandering,* In: *"River Meandering*". Elliot, C. (Ed.), ASCE, New York, PP. 952-963.
13. Hsieh, T. Y. and Yang, J. C. 2003. Investigation on the Suitability of Two Dimensional Depth Averaged Models for Bend Flow Simulation, *J. Hydraul. Eng., ASCE*, **129(8):** 597-612.
14. Johannesson, H., and parker, G. 1989a. Secondary flow in a mildly sinuous channel. *J. Hydrol. Eng*., **115(3)**: 289-308.

[DOR: 20.1001.1.16807073.2009.11.4.8.3]

15. Johannesson, H., and Parker, G. 1989b. Velocity Redistribution in Meandering Rivers. *J. Hydrol. Eng.,* **115(8)**: 1019-1039.
16. Kalkwijk, J. P. and de Vriend, H. J. 1980. Computation of the Flow in Shallow River Bends. *J. Hydraul. Res*., **18(4):**327-342.
17. Kin, J. and Moin, P. 1985. Application of Fractional-step Method to Incompressible Navier-Stokes Equations. *J. Comp. Phys.*, **59:** 308-323.
18. Leschziner, M. A. and Rodi, W. 1979. Calculation of Strongly Curved Open Channel Flow. *J. Hydrol. Div.*, *ASCE*, **105(10):** 1297-1314.
19. Lien, H. C., Hsieh, T. Y., Yang, J. C. and Yeh, K. C. 1999. Bend Flow Simulation Using 2D Depth-averaged Model. *J. hydrol. Eng.*, **125(10)**:1097-1108.
20. Mockmore, C. 1943. Flow around Bends in Stable Channels. *Trans., ASCE,* **3**: 334.
21. Mohammadzadeh Ghomi, M. and Montazeri Namin, M. 2005. Simulation of Flow with Free Surface Using Projection Method on Unstructured Triangular Finite Volume Networks, *Proc. of the 5th Iranian Hydraulic Conference*, Shahid Bahonar University of Kerman, Nov., 8-10, **2**: 861-868.
22. Molls, T., and Chaudhry, M. H. 1995. Depth-averaged Open-channel Flow Model. *J. Hydrol. Eng.,* **121(6)**: 453-465.
23. Nelson, J. and Smith, J. 1989. Evolution and Stability of Erodible Channel beds. Technical Report, American Geophysics Union, Washington, D. C..
24. Odgaard, A. J. 1989. River Meander Model. I: Development. *J. Hydrol. Eng.,* ASCE, **115(11)**: 1433_1450.
25. Rowinski, P. M., Dysarz, T. and Napiorkowski, J. J. 2004). Estimation of Longitudinal Dispersion and Storage Zone Parameters. In: "*River Flow 2004-Greco*". Carravetta and Della Morte, London.
26. Rozovskii, I. L. 1961. *Flow of Water in Bends of Open Channels*. The Israel Program for Scientific Translations, Jerusalem.
27. Shimizu, Y., Yamaguchi, H. and Itakura, T. 1990. Three Dimensional Computations of Flow and Bed Deformation. *J. Hydrol. Eng., ASCE*, **116(9)**: 1090-1108.
28. Shukhry, A. 1949. Flow around Bends in an Open Flume. *J. Hydrol. Div., ASCE*, **75**: 713.
29. Sinha, S. K., Sotiropoulos, F. and Odgaard, A. J. 1998. Three Dimensional Numerical Model for Flow through Natural Rivers. *J. Hydrol. Eng., ASCE*, **124(1)**:13-24.
30. Smith, J. 1984. A Model for Flow in Meandering Streams. *Water Resour. Res*., **20(9)**: 1301-1315.
31. Temam, R. 1991. Remark on the Pressure Boundary Condition for the Projection Method. *Theor. Comput. Fluid Dynamics*, **3**: 181-184.
32. Thein K. N. N., 1994. River Plan form Movement in an Alluvial Plain. Ph. D. Thesis, International Institute for Infrastructural, Hydraulic and Environmetal Engineering.
33. Thomson, J. J. 1876. On the Windings of Rivers in Alluvial Plains. *Proc. Roy. Soci. London*, **25**: 5-8.
34. Wu, W., Rodi, W., and Wenka, T. 2000. 3D Numerical modeling of flow and sediment transport in open channels, *J. of Hydr. Engr,* **126(1)**: 4-15.
35. Ye, J. and McCorquodale, J. A. 1997. Depth Averaged Hydrodynamic Model in Curvilinear Collocated Grid. *J. Hydrol. Eng.*, *ACSE*, **123(5)**:380-388.
36. Yen, B. C. 1965. Characteristics of Sub-critical Flow in a Meandering Channel. Ph. D. Thesis, University of Iowa, Iowa City, Iowa.

[DOR: 20.1001.1.16807073.2009.11.4.8.3]

مدل عددی دوبعدی متوسط عمقی برای جریان غیرماندگار در خم

م. م. احمدی، س. ع. ایوب زاده، م. منتظری نمین و ج. م. و. سامانی

چکیده

یک مدل عددی دوبعدی متوسط عمقی برای شبیه سازی جریان در خم کانال ها در مختصات منحنی الخط متعامد توسعه داده شد. در این مدل تاثیر جریان ثانویه با وارد کردن عبارات تنش های پراکندگی که از انتگرال گیری تفاضل بین توزیع ولقعی و توزیع متوسط عمقی در جهات جریان و جهت عرضی بدست می آیند در معادلات مومنتم، لحاظ شد. معادلات مربوطه به روش حجم کنترل گسسته سازی شد و از روش تصویری برای حل معادلات استفاده شد. نتایج حاصل از مدل با دو سری نتایج منتج از آزمایشات مقایسه شده و تطابق خوبی را نشان داد.

[DOR: 20.1001.1.16807073.2009.11.4.8.3]